



ULUSLARARASI 3B YAZICI TEKNOLOJİLERİ
VE DİJİTAL ENDÜSTRİ DERGİSİ

INTERNATIONAL JOURNAL OF 3D PRINTING
TECHNOLOGIES AND DIGITAL INDUSTRY

ISSN:2602-3350 (Online)

URL: <https://dergipark.org.tr/ij3dptdi>

THE EFFECT OF NOZZLE DIAMETER AND LAYER THICKNESS ON MECHANICAL BEHAVIOR OF 3D PRINTED PLA LATTICE STRUCTURES UNDER QUASI-STATIC LOADING

Yazarlar (Authors): Emre Demirci^{ID*}, Safa Şenaysoy^{ID}, Salih Emre Tuğcu^{ID}

Bu makaleye şu şekilde atıfta bulunabilirsiniz (To cite to this article): Demirci E., Şenaysoy S., Tuğcu S. E., “The Effect of Nozzle Diameter and Layer Thickness on Mechanical Behavior of 3D Printed PLA Lattice Structures Under Quasi-Static Loading” *Int. J. of 3D Printing Tech. Dig. Ind.*, 7(1): 105-113, (2023).

DOI: 10.46519/ij3dptdi.1256993

Araştırma Makale/ Research Article

Erişim Linki: (To link to this article): <https://dergipark.org.tr/en/pub/ij3dptdi/archive>

THE EFFECT OF NOZZLE DIAMETER AND LAYER THICKNESS ON MECHANICAL BEHAVIOR OF 3D PRINTED PLA LATTICE STRUCTURES UNDER QUASI-STATIC LOADING

Emre Demirci^a , Safa Şenaysoy^a , Salih Emre Tuğcu^a 

^aBursa Technical University, Faculty of Engineering and Natural Sciences, Department of Mechanical Engineering, TURKIYE

* Corresponding Author: emre.demirci@btu.edu.tr

(Received: 27.02.2023; Revised: 30.03.2023; Accepted: 25.04.2023)

ABSTRACT

Lattice structures are widely preferred because they have good properties such as lightness, high energy absorption capacity, and strength. Moreover, these lattice structures can be produced by utilizing a 3D printer. Therefore, this study aimed to explore the effect of the mechanical behavior of the different printing parameters on the lattice structures. Firstly, FBCC and FBCCZ lattice structures were printed with various printing parameters such as nozzle diameter of 0.25 mm-0.4 mm and layer thickness of 0.1 mm-0.15 mm. Then, quasi-static compression tests were performed to determine the mechanical behavior of lattice structures. Force-displacement behavior, equivalent elastic modulus, and energy absorption capabilities of lattice structures printed with different parameters were calculated from the results of the quasi-static compression test. According to the results, it was observed that the mechanical behavior was significantly affected when the nozzle diameter and layer thickness were changed. It was determined that the strength and energy absorption of the structures printed with a nozzle diameter of 0.25 mm and a layer thickness of 0.15 mm were decreased. In addition, it was observed that the influence of the printing parameters on the mechanical performance can be different according to the lattice type and lattice rod diameter. The combination of small nozzle diameter and high layer thickness caused a decrease in mechanical strength in both lattice types. Moreover, the highest specific energy absorption value was obtained in the samples printed with a 0.4 mm nozzle diameter and a 0.15 mm layer thickness.

Keywords: Lattice Structure, Printing Parameters, Mechanical Behavior, 3D Printing, PLA.

1. INTRODUCTION

Industrial revolutions undoubtedly have a great impact on our lives. When these revolutions are examined, it is observed that knowledge is constantly developing and changing. With each development, a higher quality, faster, lower cost, more functional, safer, and more accurate industrialization is aimed. 3D printing technology, which comes to the fore when the cornerstones of the sector are examined and has become the focus of attention of a wide segment, is an important technological development that will shape the current and future manufacturing process. The additive manufacturing method is universally used in various fields from defense to the aerospace industry, from the automotive to the biomedical sector [1-4]. Thanks to the developments in the field of additive manufacturing, complex

structures can be produced with different methods for the desired material. Some of these methods can produce 3D structures in layers by melting powder or filament materials, solidifying liquid materials, or injecting the material [5,6].

Additive manufacturing employs a variety of techniques, and among them, Fused Deposition Modeling (FDM) is one of the most widely utilized and popular processes. With the FDM process, the thermoplastic filament material is melted and combined layer by layer with a moving nozzle to obtain the desired geometry [7,8]. In addition, different types of polymeric materials such as Polylactic acid (PLA), Polypropylene (PP), Acrylonitrile butadiene styrene (ABS), Polycarbonate (PC), and composites can be used in this method and thus

structures can be produced according to different strength and thermal requirements [9]. In addition, the mechanical behavior of FDM-printed structures is influenced by a variety of manufacturing factors. The literature predominantly focuses on investigating the influence of manufacturing parameters on the mechanical characteristics of tensile test specimens printed via FDM [10-12]. Many studies show that various parameters such as layer thickness [13,14], building direction [15,16], infill densities [17-19], nozzle diameter [20], and printing speed [20,21] have notable effects on the mechanical features of FDM printed structures.

One of the most significant gains of additive manufacturing to production technologies is the ability to easily print structures that cannot be produced by traditional production methods. In this sense, lattice structures are prominent examples of situations where strength and lightness are desired together. Many different lattice structures have drawn the attention of researchers for various reasons. Lattice structures can be optimized for specific applications using generative design software, allowing for greater material efficiency and reduced weight without sacrificing mechanical performance [22, 23]. This makes them ideal for a range of industries, including aerospace, automotive, and medical, where weight reduction is critical for improved performance and efficiency. In addition, lattice structures provide a high level of design flexibility and customization, enabling the production of intricate geometries that would be challenging or unfeasible with conventional manufacturing techniques. Gürkan and Sağbaşı [24] investigated Ti6Al4V star, octahedral, and dodecahedron lattice structures for biomedical applications. In other studies, a 25% weight reduction was observed in the engine hood by using pyramidal lattice structures and 19% in gears thanks to honeycomb lattice structures [25,26]. Nasrullah et al. [27] studied the crashworthiness of eleven different types of lattice structures. Poyraz et al. [28] numerically investigated the elastic and physical properties of simple cubic, face-centered cubic, and body-centered lattice structures. Tang et al. [29] examined how the mechanical properties of PLA lattice structures are impacted by changes in both printing speed and printing temperature.

In this paper, equivalent young's modulus and energy absorption characteristics of face-and-body-centered cubic (FBCC) and FBCC with Z-strut (FBCCZ) lattice structures with different production and structural parameters were investigated.

2. MATERIALS AND METHODS

2.1. Lattice Design

For lattice structure design, cubic structure, one of the most widely used types in the research studies, was considered. FBCC and FBCCZ unit cells, which were determined to have superior mechanical properties among cubic-based structures in the literature review, were selected for the lattice structure design [30, 31]. The authors selected two distinct cell types to ascertain whether the impact of diverse parameters on mechanical properties remains constant, irrespective of the unit cell type utilized. The computer-aided design (CAD) models of the unit cell and lattice structures that were employed in this research were presented in Figure 1.

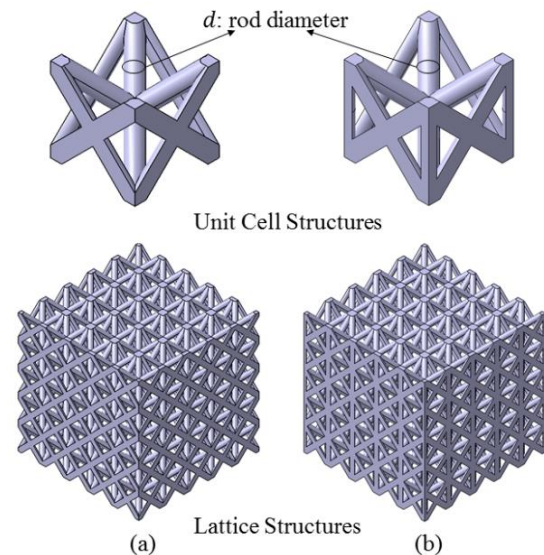


Figure 1. CAD model of the unit cell and lattice structures; (a) FBCC, (b) FBCCZ.

The unit cells were designed as 8x8x8 mm, as in many studies in the literature [32,33]. As the number of repetitions of the unit cell increases, the lattice structures better satisfy the periodic boundary conditions. On the other hand, the high number of repetitions of the unit cell leads to long printing time. Thus, the lattice structures were composed of 5x5x5 cells. The rod (strut) diameters of unit cells were determined as 0.75 mm and 0.1 mm as structural parameters. In this

way, a total of 4 different lattice structures, 2 FBCC, and 2 FBCCZ, were designed.

2.2. 3D Printing with FDM

The designed lattice structure CAD files were converted to STL format for manufacturing with FDM. The Ultimaker 3 Extended 3D printer was used for the additive manufacturing of lattice samples as shown in Figure 2. Ultimaker PLA filament with a diameter of 2.85 mm was utilized as the material. The mechanical properties of the PLA material for flat printing orientation were given in Table 1.

Table 1. Properties of the PLA material.

Property	Value	Unit
Young's modulus	3250	MPa
Yield stress (tensile)	52.5	MPa
Breaking stress (tensile)	45.5	MPa
Maximum elongation	7.8	%
Flexural modulus	3019	MPa



Figure 2. Manufacturing of lattice specimen with the 3D printer.

In order to print the lattice samples on the 3D printer, adjustment of the printing parameters and the G-code transformation of the STL data were performed with Cura software. All lattice samples, except for variations in nozzle diameter and layer thickness, were printed using constant printing parameters as listed in Table 2.

Table 2. Printing parameters.

Parameter	Value
Nozzle diameter	0.25 mm - 0.4 mm
Printing speed	30 mm/s
Build plate temperature	60 °C
Nozzle temperature	200 °C
Infill density	100 %
Filament diameter	2.85 mm
Layer thickness	0.1 mm – 0.15 mm

This study's goal was to find out how variations in nozzle diameter and layer thickness, as production parameters, impact the mechanical performance of lattice structures. Accordingly, two nozzle diameters, 0.4 mm, and 0.25 mm were selected utilizing diverse print cells that are compatible with the 3D printer. Also, as another production parameter, layer thicknesses were determined as 0.1 mm and 0.15 mm. Layer thicknesses were chosen considering the limitations of nozzle diameters for production. Table 3 lists the notation describing the combination of production and design parameters used in this research. A and B indicate the rod diameter as 0.75 mm and 1 mm, X and Y indicate the nozzle diameter as 0.4 mm and 0.25 mm, and 1 and 2 indicate layer thickness as 0.1 mm and 0.15 mm.

Table 3. Specimen combinations notation.

Specimen ID	Rod dia. (mm)	Nozzle dia. (mm)	Layer thickness (mm)
FBCC_AX1	0.75	0.4	0.1
FBCC_BX1	1.0	0.4	0.1
FBCC_AY1	0.75	0.25	0.1
FBCC_BY1	1.0	0.25	0.1
FBCC_AX2	0.75	0.4	0.15
FBCC_BX2	1.0	0.4	0.15
FBCC_AY2	0.75	0.25	0.15
FBCC_BY2	1.0	0.25	0.15
FBCCZ_AX1	0.75	0.4	0.1
FBCCZ_BX1	1.0	0.4	0.1
FBCCZ_AY1	0.75	0.25	0.1
FBCCZ_BY1	1.0	0.25	0.1
FBCCZ_AX2	0.75	0.4	0.15
FBCCZ_BX2	1.0	0.4	0.15
FBCCZ_AY2	0.75	0.25	0.15
FBCCZ_BY2	1.0	0.25	0.15

Variable parameters, such as nozzle diameter and layer thickness, were observed to affect the appearance of printed samples in a non-macroscopic manner. Hence, the pictures of FBCC_BX1 and FBCCZ_BX1 were given in Figure 3 as examples of printed samples.

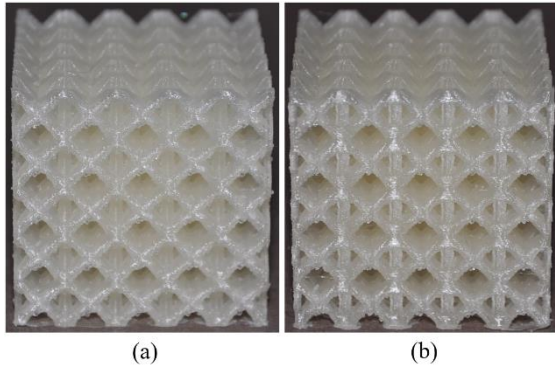


Figure 3. Example pictures of printed lattice structures: a) FBCC_BX1, b) FBCCZ_BX1.

2.3. Experimental Setup

The Shimadzu AG-X universal testing machine with a 250 kN load cell was used for the compression test of the lattice specimens. Experimental tests were carried out at room temperature. Compression speed was applied as 1 mm/min to provide quasi-static condition. As seen in Figure 4, the lattice specimen was placed on the fixed base table and subjected to compression load with the movable fixture. During the test, data were collected with TRAPEZIUM X software, and force-stroke values were obtained.

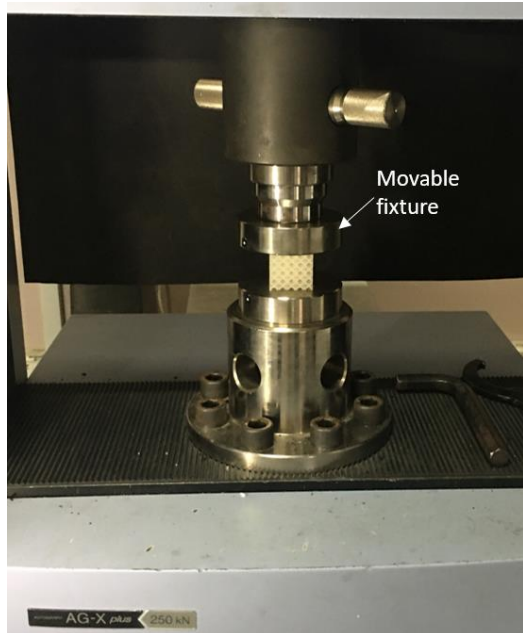


Figure 4. Compression test setup.

3. RESULTS AND DISCUSSION

3.1. Force-Displacement Behavior

In order to observe how production and structural parameters affect the crushing behavior of lattice structures, force-displacement curves of all samples were plotted in the same graph. As a result of the material's accumulation due to deformation during the test, the reaction forces increased significantly towards the end of the test, but this increase was not caused by the characteristics of the lattice structure. Therefore, all the graphs were plotted for 20 mm deformation. Figure 5 illustrates the force-displacement behavior of all FBCC samples.

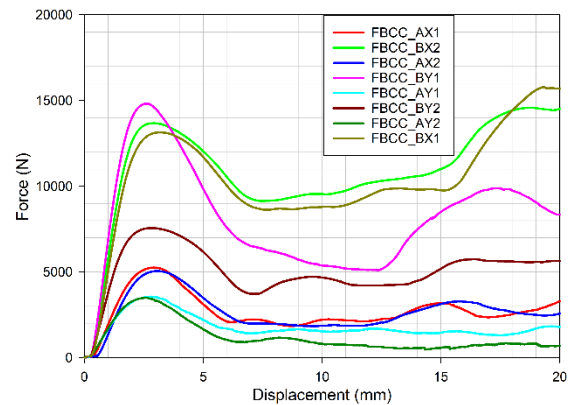


Figure 5. Force-displacement curves of FBCC samples.

It was seen that all FBCC samples show a linear behavior in reaction force increase to the first peak. It was observed that the first peak forces of the samples with a rod diameter of 1 mm were higher as expected. Samples FBCC_BX1 and FBCC_BX2 with layer thickness of 0.1 and 0.15 mm printed with a 0.4 mm nozzle exhibited similar behavior. However, it was observed that the curve characteristics of the FBCC_BY1 and FBCC_BY2 samples printed with a 0.25 nozzle were very different. The compressive strength of the 1 mm rod diameter FBCC_BY2 sample, which includes the combination of small nozzle diameter and high layer thickness, was considerably lower than the other 1 mm rod diameter samples. On the other hand, examining the results of the samples with a rod diameter of 0.75 mm, it was found that the compressive strength of the samples printed with a 0.4 mm nozzle was higher than that of those printed with a 0.25 mm nozzle. In addition, it was observed that the effect of the layer thickness was not much for the 0.4 mm nozzle, whereas the low

layer thickness value increased the strength in the samples printed with the 0.25 mm nozzle.

It was investigated whether parameter changes in the FBCCZ lattice structure gave similar results. Figure 6 illustrates the force-displacement behavior of all FBCCZ samples.

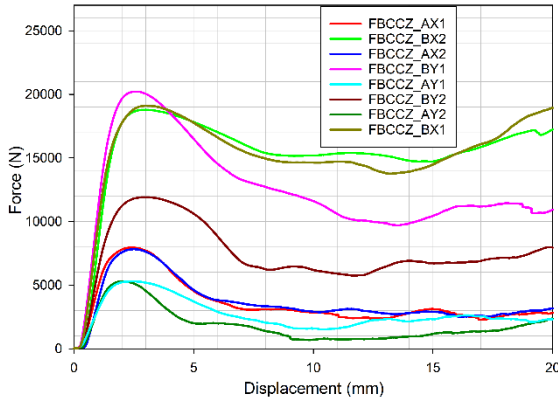


Figure 6. Force-displacement curves of FBCCZ samples.

When the graph is examined, it was seen that all FBCCZ samples have higher compressive strength compared to FBCC samples printed with the same parameters, thanks to the Z strut structures. Among the FBCCZ samples with a rod diameter of 1 mm, the strength of the sample printed with a nozzle with a diameter of 0.25 mm and a layer thickness of 0.15 mm is significantly lower than the others. Similar to the findings for the FBCC structures, it was observed that the structures printed with a 0.4 mm nozzle exhibited greater strength, particularly for the 0.75 mm rod diameter samples.

3.2. Equivalent Elastic Modulus

Elastic modulus is defined as resistance against deformation in the linear-elastic region and is one of the essential material properties. The equivalent elastic modulus approach is widespread to characterize the mechanical behavior of lattice structures. The lattice structure is considered as a continuous medium when calculating the equivalent elastic modulus. The equivalent elastic modulus was determined by using linear regions of force-displacement curves in Figures 5 and 6. Results of equivalent elastic modulus were given in Figure 7.

Figure 7 shows that FBCCZ lattice structures have higher equivalent elastic modulus than FBCC lattice structures since FBCCZ lattice

structures contain additional vertical struts in the compression test direction. As the bar diameter changes from 0.75 mm to 1.00 mm, the porosity ratio decreases, and the equivalent elastic modulus increases for both FBCC and FBCCZ structures. Therefore, lattice structures with a rod diameter of 1.0 mm exhibit more robust mechanical behavior. In lattice structures with a rod diameter of 0.75 mm, as the nozzle diameter decreases, the equivalent elastic modulus decreases for each lattice structure and layer thickness.

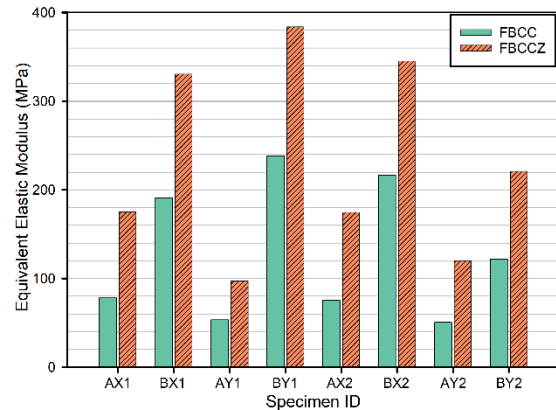


Figure 7. Equivalent elastic modulus of FBCC and FBCCZ samples.

It was determined that the model with the highest equivalent elastic modulus among all samples was the FBCCZ_BY1 model with a value of 383.79 MPa. Furthermore, among the FBCC lattice samples, the BY1 model reached the highest equivalent elastic modulus value. The lowest equivalent elastic modulus was obtained as 50.57 MPa for the FBCC_AY2 model. On the other hand, for the FBCCZ lattice type, the lowest value was obtained in the AY1 model. In the circumstances, lattice samples printed with 0.75 mm rod diameter and 0.25 mm nozzle diameter appear to be the worst combination for the equivalent elastic modulus. In combinations where the rod and nozzle diameters were kept constant and the layer thickness changed, no significant changes were observed between the results of the AX1-AX2, BX1-BX2, and AY1-AY2 models. On the contrary, increasing the layer thickness to 0.15 mm at 0.1 mm in the samples in which the lattice structures with a rod diameter of 1 mm were printed with a 0.25 mm nozzle resulted in a decrease of more than 50% in the equivalent elastic modulus.

3.3. Energy Absorption Characteristics

Determining a lattice structure's capacity to absorb energy is one of the important indicators used throughout the mechanical evaluation of that structure. The total energy absorption (E_T) is defined as the area under the force-displacement graph and is expressed as shown in Equation (1).

$$E_T = \int_0^{\delta} F(x)dx \quad (1)$$

where δ is the total displacement during the compression test and F is the crushing force. In cases where the weight of a structure is also

important, the total energy absorption index may not be an adequate comparison or evaluation parameter [34-35]. The specific energy absorption (SEA) value, which additionally considers the structure's mass, can be applied in this circumstance. SEA can be calculated by the formulation in Equation (2).

$$SEA = E_T/m \quad (2)$$

In this formula, the mass of the structure is denoted by m . The total energy absorption and SEA values obtained as a result of the test applied to all samples were given in Figure 8.

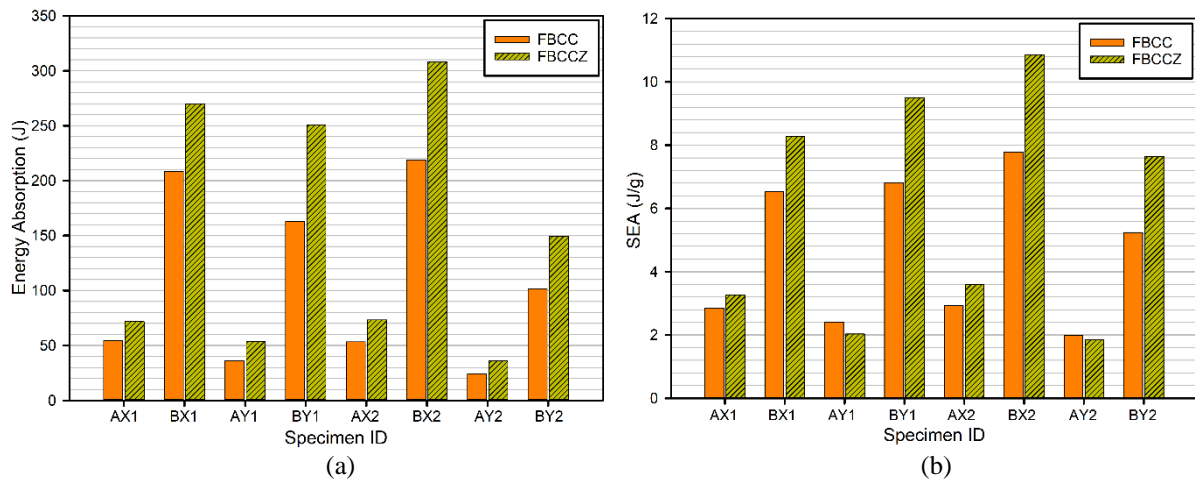


Figure 8. Comparison of lattice samples: a) total energy absorption values, b) specific energy absorption values.

When Figure 8a is examined, it is seen that the Z-supported structures absorb more energy. The structures that absorb the most and the least energy were FBCCZ_BX2 and FBCC_AY2 with the values of 380.18 J and 23.97 J, respectively. It is also an expected result that structures with a 1 mm rod diameter absorb more energy than structures with a 0.75 mm rod diameter. Among the structures with a rod diameter of 1 mm, the combination that absorbed the most energy was the BX2 samples produced with a layer thickness of 0.15 mm and a nozzle diameter of 0.4 mm for both lattice types. When the results of 0.75 mm rod diameter structures are examined, the layer thickness did not have a significant effect on energy absorption in the samples printed with 0.4 mm nozzle diameter, while the lower layer thickness gave better results in the samples printed with 0.25 mm nozzle diameter. Considering the nozzle diameter as the only variable, samples printed with a 0.4 mm nozzle absorbed more energy than samples printed

with a 0.25 mm nozzle for both FBCC and FBCCZ lattice structures.

In the production of thermoplastic materials with additive manufacturing, the mass of the lattice structure is affected by the production parameters [36]. It was necessary to take into account the change in the mass of the structures caused by the layer thickness and nozzle diameter variables. Therefore, in addition to total energy absorption, SEA values were calculated and shown in Figure 8b. Similar to the total energy absorption graph, the highest SEA value was obtained in the FBCCZ_BX2 as 10.85 J/g. Although it was observed that the FBCCZ structures absorb more energy in general, it was determined that the FBCC structure reaches a higher SEA value in the AY1 and AY2 models with the combination of 0.75 mm rod diameter and 0.25 mm nozzle diameter. This was due to the lighter mass of the samples printed with the 0.25 mm nozzle compared to the 0.4 mm nozzle. On the other side, it was found that increasing the layer thickness led to

the creation of lighter PLA structures, resulting in higher SEA values. While the structure with the worst performance in total energy absorption was FBCC_AY2, when the SEA values were considered, the lowest value belongs to the FBCCZ_AY2 structure with 1.85 J/g.

4. CONCLUSIONS

In this research, the mechanical performances of FBCC and FBCCZ lattice structures printed with different parameters using FDM under the quasi-static compression test were investigated. Two different layer thicknesses and two different nozzles were considered as printing parameters, and the effects of these parameters on structures with 0.75 mm and 1 mm rod diameters were evaluated. The experimental study's results were condensed and presented in the following manner:

- The Z structure added to the FBCC structure increased the initial reaction force under loading by an average of 48% in samples with a 0.75 mm rod diameter and by an average of 44% in samples with a bar diameter of 1 mm.
- Among the lattice structures with a rod diameter of 1 mm, the structures with the lowest strength were the samples printed with a nozzle diameter of 0.25 mm and a layer thickness of 0.15 mm. The initial reaction force of the samples printed with this combination decreased by about 83% and 62% for FBCC and FBCCZ, respectively, compared to the other samples.
- When the effect of production parameters on the equivalent elastic modulus was examined, it was observed that the effects changed according to the rod diameter of the lattice structures.
- Regardless of the lattice type and rod diameter, the best results in total energy absorption were obtained with the combination of 0.4 mm nozzle diameter and 0.15 mm layer thickness. When only the nozzle diameters were compared, the structures printed with 0.4 mm nozzle in all sample types absorbed more energy.
- It was determined that the combinations of 0.15 mm layer thickness - 0.4 mm nozzle diameter and 0.1 mm layer thickness - 0.25 mm nozzle diameter were more effective in terms of energy absorption.
- The effect of printing parameters was more notable on SEA. While the total energy absorbed by FBCC and FBCCZ structures with 1 mm rod diameter was approximately 4.1 times higher than for 0.75 mm diameter structures, this rate decreased to 2.6 for FBCC structures and 3.4 for FBCCZ structures in SEA.
- The combination of small nozzle diameter and high layer thickness caused a decrease in mechanical strength in both lattice types.
- It was determined that the effect of the nozzle diameter on the mechanical properties is more significant compared to the other parameters.
- Although there are different research studies examining the printing parameters, this study showed that the effect of the parameters may have different results depending on the lattice type and porosity ratio.

ACKNOWLEDGES

This study was supported by the Bursa Technical University Scientific Research Project Units (Project No: 211N003).

REFERENCES

1. Vilardell, A.M., Takezawa, A., Du Plessis, A., Takata, N., Krakhmalev, P., Kobashi, M., Yadroitsev, I., "Topology optimization and characterization of Ti6Al4V ELI cellular lattice structures by laser powder bed fusion for biomedical applications", *Materials Science and Engineering: A*, Vol. 766, 138330, 2019.
2. Özel, Ş., Zeren, M., Alp, Ç.N., "Application Of Layered Manufacturing Technology With 3d Printers In Automotive Industry", *International Journal of 3D Printing Technologies and Digital Industry*, Vol. 4, Issue 1, Pages 18-31, 2020.
3. Özsoy, K., Duman, B., Gültekin, D.İ., "Metal part production with additive manufacturing for aerospace and defense industry", *International Journal of Technological Sciences*, Vol.11, Issue 3, Pages 201-210, 2019.
4. Aslan, B., Yıldız, A.R., "Optimum design of automobile components using lattice structures for additive manufacturing", *Materials Testing*, Vol. 62, Issue 6, Pages 633-639, 2020.
5. Bhushan, B., Caspers, M., "An overview of additive manufacturing (3D printing) for microfabrication", *Microsystem Technologies*, Vol. 23, Issue 4, Pages 1117-1124, 2017.

6. Ngo, T. D., Kashani, A., Imbalzano, G., Nguyen, K. T., Hui, D., “Additive manufacturing (3D printing): A review of materials, methods, applications and challenges”, *Composites Part B: Engineering*, Vol. 143, Pages 172-196, 2018.
7. Mohamed, O. A., Masood, S. H., Bhowmik, J. L., “Optimization of fused deposition modeling process parameters: a review of current research and future prospects”, *Advances in Manufacturing*, Vol. 3, Issue 1, Pages 42-53, 2015.
8. Başçı, Ü.G., Ymanoğlu, R., “Yeni Nesil Üretim Teknolojisi : FDM ile Eklemeli İmalat”, *International Journal of 3D Printing Technologies and Digital Industry*, Vol. 5, Issue 2, Pages 339-352, 2021.
9. Dezaki, M. L., Ariffin, M. K. A. M., Hatami, S., “An overview of fused deposition modelling (FDM): Research, development and process optimization”, *Rapid Prototyping Journal*, Vol. 27, Issue 3, Pages 562-582, 2021.
10. Tuğcu, S. E., Şenaysoy, S., Demirci, E., “Effect of Build Orientation and Layer Thickness on Tensile Properties of FDM Printed PLA and PA Materials”, 1st International Materials Engineering and Advanced Manufacturing Technologies Congress, Pages 105-110, İstanbul, 2022.
11. Altan, M., Eryildiz, M., Gumus, B., Kahraman, Y., “Effects of process parameters on the quality of PLA products fabricated by fused deposition modeling (FDM): surface roughness and tensile strength”, *Materials Testing*, Vol. 60, Issue 5, Pages 471-477, 2018.
12. Hsueh, M. H., Lai, C. J., Chung, C. F., Wang, S. H., Huang, W. C., Pan, C. Y., ... & Hsieh, C. H., “Effect of Printing Parameters on the Tensile Properties of 3D-Printed Polylactic Acid (PLA) Based on Fused Deposition Modeling”, *Polymers*, Vol. 13, Issue 14, 2387, 2021.
13. Kamaal, M., Anas, M., Rastogi, H., Bhardwaj, N., Rahaman, A., “Effect of FDM process parameters on mechanical properties of 3D-printed carbon fibre-PLA composite”, *Progress in Additive Manufacturing*, Vol. 6, Issue 1, Pages 63-69, 2021.
14. Samykano, M., Selvamani, S. K., Kadirgama, K., Ngui, W. K., Kanagaraj, G., Sudhakar, K., “Mechanical property of FDM printed ABS: influence of printing parameters”, *The International Journal of Advanced Manufacturing Technology*, Vol. 102, Issue 9, Pages 2779-2796, 2019.
15. Camargo, J. C., Machado, Á. R., Almeida, E. C., Silva, E. F. M. S., “Mechanical properties of PLA-graphene filament for FDM 3D printing”, *The International Journal of Advanced Manufacturing Technology*, Vol. 103, Issue 5, Pages 2423-2443, 2019.
16. Popescu, D., Zapciu, A., Amza, C., Baci, F., Marinescu, R., “FDM process parameters influence over the mechanical properties of polymer specimens: A review”, *Polymer Testing*, Vol. 69, Pages 157-166, 2018.
17. Fernandez-Vicente, M., Calle, W., Ferrandiz, S., Conejero, A., “Effect of infill parameters on tensile mechanical behavior in desktop 3D printing”, *3D printing and additive manufacturing*, Vol. 3, Issue 3, Pages 183-192, 2016.
18. Dobos, J., Hanon, M. M., Oldal, I., “Effect of infill density and pattern on the specific load capacity of FDM 3D-printed PLA multi-layer sandwich”, *Journal of Polymer Engineering*, Vol. 42, Issue 2, Pages 118-128, 2021.
19. Eryildiz, M., “The effects of infill patterns on the mechanical properties of 3D printed PLA parts fabricated by FDM”, *Ukrainian Journal of Mechanical Engineering and Materials Science*, Vol. 7, Pages 1-8, 2021.
20. Solomon, I. J., Sevel, P., Gunasekaran, J., “A review on the various processing parameters in FDM”, *Materials Today: Proceedings*, Vol. 37, Pages 509-514, 2021.
21. Algarni, M., Ghazali, S., “Comparative study of the sensitivity of PLA, ABS, PEEK, and PETG’s mechanical properties to FDM printing process parameters”, *Crystals*, Vol. 11, Issue 8, 995, 2021.
22. Pan, C., Han, Y., Lu, J., “Design and optimization of lattice structures: A review”, *Applied Sciences*, Vol. 10, Issue 18, 6374, 2020.
23. Baykasoğlu, A., Baykasoğlu, C., Cetin, E., Multi-objective crashworthiness optimization of lattice structure filled thin-walled tubes”, *Thin-Walled Structures*, Vol. 149, 106630, 2020.
24. Sağbaş, B., Gürkan, D., “Additively manufactured Ti6Al4V lattice structures for biomedical applications”, *International Journal of 3D Printing Technologies and Digital Industry*, Vol. 5, Issue 2, Pages 155-163, 2021.
25. Yin, S., Chen, H., Wu, Y., Li, Y., Xu, J., “Introducing composite lattice core sandwich structure as an alternative proposal for engine hood”, *Composite Structures*, Vol. 201, Pages 131-140, 2018.
26. Kulangara, A. J., Rao, C. S. P., Bose, P. S. C. “Generation and optimization of lattice structure on

a spur gear”, *Materials Today: Proceedings*, Vol. 5, Issue 2, Pages 5068-5073, 2018.

27. Nasrullah, A. I. H., Santosa, S. P., Dirgantara, T., “Design and optimization of crashworthy components based on lattice structure configuration”, *Structures*, Vol. 26, Pages 969-981, 2020.

28. Poyraz, Ö., Bilici, B. E., Gedik, Ş. C. “Numerical Investigations and Benchmarking of The Physical and Elastic Properties of 316L Cubic Lattice Structures Fabricated by Selective Laser Melting” *International Journal of 3D Printing Technologies and Digital Industry*, Vol. 6, Issue 1, Pages 13-22, 2022.

29. Tang, C., Liu, J., Yang, Y., Liu, Y., Jiang, S., Hao, W., “Effect of process parameters on mechanical properties of 3D printed PLA lattice structures”, *Composites Part C: Open Access*, Vol. 3, 100076, 2020.

30. Seharing, A., Azman, A. H., Abdullah, S., “A review on integration of lightweight gradient lattice structures in additive manufacturing parts”, *Advances in Mechanical Engineering*, Vol. 12, Issue 6, 1687814020916951, 2020.

31. Zhang, X. Z., Leary, M., Tang, H. P., Song, T., Qian, M., “Selective electron beam manufactured Ti-6Al-4V lattice structures for orthopedic implant applications: Current status and outstanding challenges” *Current Opinion in Solid State and*

Materials Science, Vol. 22, Issue 3, Pages 75-99, 2018.

32. Cao, X., Xiao, D., Li, Y., Wen, W., Zhao, T., Chen, Z., Fang, D., “Dynamic compressive behavior of a modified additively manufactured rhombic dodecahedron 316L stainless steel lattice structure”, *Thin-Walled Structures*, Vol. 148, 106586, 2020.

33. Mancini, E., Utzeri, M., Sasso, M., “Investigation on Homogeneous Modeling of Gyroid Lattice Structures: Numerical Study in Static and Dynamic Conditions” *Key Engineering Materials*, Vol. 926, Pages 2119-2126, 2022

34. Yildirim, A., Demirci, E., Karagöz, S., Özcan, Ş., Yildiz, A.R., “Experimental and numerical investigation of crashworthiness performance for optimal automobile structures using response surface methodology and oppositional based learning differential evolution algorithm”, *Materials Testing*, Vol. 65, Issue 3, Pages 346-363, 2023.

35. Albak, E. İ., “Optimization for multi-cell thin-walled tubes under quasi-static three-point bending”, *Journal of the Brazilian Society of Mechanical Sciences and Engineering*, Vol. 44, Issue 5, 207, 2022.

36. Butt, J., Bhaskar, R., Mohaghegh, V., “Analysing the effects of layer heights and line widths on FFF-printed thermoplastics”, *The International Journal of Advanced Manufacturing Technology*, Vol. 121, Issue 11-12, Pages 7383-7411, 2022.